CONFORMATION AND DIFFUSION PROPERTIES OF POLYVINYL ALCOHOL AND POLYVINYLPYRROLIDONE MOLECULES

Y. G. Groda[a1], V. S. Vikhrenko[a],
A. H. Poghosyan[b], P. K. Hakobyan[b], L. H. Arsenyan[b], A. A. Shahinyan[b]

[a] *Belarusian State Technological University, 13a Sverdlova str., Minsk 220006, Belarus*
[b] *International Scientific-Educational Center of National Academy of Sciences of the Republic of Armenia, 24d Marshal Baghramyan ave., Yerevan 0019, Armenia*

ABSTRACT

Molecular dynamics simulations have been carried out on the polyvinyl alcohol (PVA) and the polyvinylpyrrolidone (PVP) water solutions to reveal their interaction mechanisms and conformation dynamics. The 100 ns simulation was done on each system, and calculations of structural parameters were performed using GROMACS software package. The full trajectory analysis discloses the structural and dynamic aspects of both polymers, and their globular structures are determined. The parameters that determine relative position of monomers are selected. It was found that the PVA molecule is a globule of almost spherical shape, while the other polymer has elongated shape. The studied properties indicate that the planes of separate monomers are chaotically distributed, while the angles between the nearest carbon bonds are approximately constant. The comparison of the end to end distances and the gyration radii demonstrates that the backbones of both polymers cannot be considered as ideal Gaussian chains. The procedure to describe a globule rotational motion is suggested. The translational and rotational diffusion coefficients were found to differ significantly between two polymers, as well as deviate from the hydrodynamic estimations.

Key words: *PVA – polyvinyl alcohol; PVP – polyvinylpyrrolidone; MD – molecular dynamics; PME method – particle mesh Ewald method; NVT ensemble – constant number of particles-volume-temperature ensemble; NPT – constant number of particles-pressure-temperature ensemble*

INTRODUCTION

The polymers are of great interest from both academic and industrial point of view, first of all, due to applications in pharmaceutics, food processing, detergent, paint production, etc. [1, 2]. Polymers are the chemical compounds of a high molecular weight and consist of a large number of repeating structural units (monomers). Synthetic and natural polymers give unique possibility to design new medical products, and also are widely applied in various areas of a science and in the industry [2–4].

Polyvinyl alcohol (PVA) is a water-soluble polymer synthesized by alkali/acid hydrolysis of complex polyvinyl ethers. Alongside with experimental studies [5,6], recently, the computational experiments have been done on the PVA oligomer in very diluted aqueous solution, where the different force field sets were compared [7]. Using the molecular dynamics (MD) Rossinsky et al. have considered the melts of short poly(vinyl alcohol) (PVA) oligomers [8]. The polymer-water interaction, the polymer connectivity and the water dynamics at various temperatures has been recently investigated by MD and incoherent neutron scattering methods [9].

Polyvinyl pyrrolidone (PVP) is a widely used synthetic polymer [4, 6], consisting of a pyrrole bound to vinylic backbone. The possible effects of PVP on the properties of liquid water and water in clathrate hydrate have been studied using MD simulations [10]. The amorphous system of indomethacin and PVP and their molecular interactions explored by MD simulations has been reported as well [11].

In this paper we report the results of the study of the dynamical and conformational features of PVA and PVP in water solution. We have demonstrated that the PVA molecule has a globular structure, which is in agreement with experimental observations [3]. We used the method of molecular dynamics simulation, which makes it possible to examine in detail the conformation structure at atomistic scale and provide information about the dynamical features of the mentioned complex systems that are not accessible by any of known experimental methods.

THE MODEL CONSTRUCTION AND SIMULATION DETAILS

Both systems (PVA/water and PVP/water) were designed in 3 steps: first, the molecules of monomers (PVA, PVP) have been built (*Fig. 1*) using Hyperchem (Hypercube Inc.) software on the basis of available crystallographic parameters (length of covalent bonds, covalent and dihedral angles, etc.) and replicated into vacuum to get 1024 and

---

[1] Corresponding author: e-mail address: groda@belstu.by; tel. +375(17)3273035 (Y.G. Groda)

408 monomers for the PVA and PVP molecules, respectively (with ~40000 *g/mol* molar weight for each polymer), correspondingly. Both polymers contain backbones formed by carbon atoms and each monomer contains two backbone carbons. Two carbon atoms in the monomers are not equivalent to each other. One of them (C1) forms the bond with the oxygen (in PVA) or nitrogen (in PVP) atom and the other (C2) is bound to the carbon C1 atom of another monomer. Thus, the carbon atoms backbone mainly defines the macromolecule space structure, and OH and NC_4H_6O groups are joined to each second carbon atom of the backbone. The partial charges were set using Dundee PRODRG server and modified according to [12, 13].

At the second step the studied polymers were subjected to 5000 steps energy minimization to avoid unphysical

(a)   (b)

Fig. 1. Monomer units of the PVP (*a*) and PVA (b) molecules.

contacts. At the third step each polymer was inserted into the water bulk with 31 000 water molecules of TIP3P water model [13, 14]. Thus, two systems were obtained – PVA/water and PVP/water – with corresponding weight ratio $C_{PVA}/C_{water} = C_{PVP}/C_{water} \cong 1/12$. The cubic box with the box side of around 10 nm and periodic boundary conditions were used.

The temperature and pressure of both systems was set to 300 K and 1 atm. The control of the pressure and temperature was done by using coupling Berendsen method [15] and V-rescale algorithm [16]. The particle mesh Ewald (PME) method [17, 18] with the tolerance of 10^{-5} was used for long-range electrostatic interactions and the cut-off of van der Waals forces were at 14 Å. The bonds were fixed at their equilibrium distances using Lincs algorithm [19], the coordinates and velocities were saved every 0.1 ns, and the molecular graphics were built using VMD packages. After the energy minimization (5000 steps with steepest descent algorithm for both systems), each of the final systems were subjected to 5 ns MD equilibration simulation run in NVT ensemble, with 1 fs time step. The final 100 ns MD simulations were carried out with 2 fs time step in NPT ensemble. The simulations and energy minimizations were performed using GROMACS 4.6.1 [14] software code with GROMOS53a4 united-atom force field. The entire simulations were performed on ArmGrid (www.grid.am) infrastructure using parallel processors.
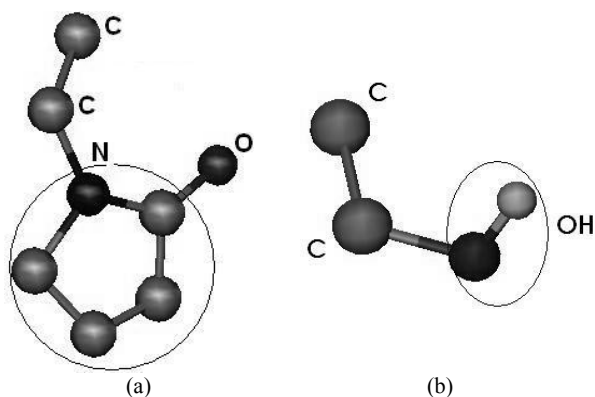
THE SIMULATION RESULTS AND DISCUSSION

The results of the conformation evolution of the compounds are presented in *Fig. 2*.

Analysis of the molecular conformation evolution indicates the trend to form more compact structures. The PVA molecule, having start configuration close to the cylindrical one, becomes close to a sphere after the first 15–25 ns of MD run, whereas the PVP molecule passed to more compact elongated body. It is evident that this difference in the initial and the final molecular configurations is due to the difference of the atomic groups attached to the backbones (a small OH in PVA and bulky NC_4H_6O in PVP).

The compaction process of the polymers can be characterized by evolution of the gyration radius (*Fig. 3*) that was calculated according to the following expression:

$$R_g^2 = \frac{1}{N}\sum_{i=1}^{N} R_i^2(t) \tag{1},$$

where $R_i(t)$ is the distance between the center of mass of *i*-th monomer and that of the whole polymer, *N* is the total number of monomeric units.

The gyration radius of the PVP molecule decreases strongly in few nanoseconds while for the PVA molecule this decrease is not so pronounced. The initial polymer configurations were taken after energy minimization at zero temperature and vacuum conditions. It is worth to note that the compaction proceeds due to interactions of the polymer molecules with the water environment at nonzero pressure. The gyration radius of the PVP molecule decreases more significantly since its initial configuration was strongly dispersed. The gyration radius evolution for both molecules can be approximated by an exponential function

$$i = i_\infty + k\exp(-t/\tau) \tag{2}.$$

The gyration radius stationary values (i_∞) were found to be 2.04 and 2.26 nm and the relaxation times (τ) are 69 and 175 ns for the PVA and PVP molecules, respectively. The relaxation time of the PVP molecule was calculated on the time interval 2–100 ns that avoids fast initial compaction.

The end-to-end distance of the polymers was calculated according to the expression:

$$R_e(t) = \left| \boldsymbol{R}_{start}(t) - \boldsymbol{R}_{end}(t) \right| \tag{3}.$$

where $\boldsymbol{R}_{start}(t)$ and $\boldsymbol{R}_{end}(t)$ are the corresponding positions of the first and last monomers centers of mass.

The end-to-end distances for the PVA and PVP molecules are shown in *Fig. 4*. The mean square values of the end-to-end distances are 8.33 and 12.9 nm^2 for the former and for the latter, respectively. The ratio of the end-to-end distance

to the gyration radius is 1.46 for PVA and 1.66 for PVP. These values are considerably smaller than those for a Gaussian chain ($\sqrt{6} \approx 2.45$) [20]. The ratio $<R_e^4>/<R_e^2>^2$ is 1.05 for PVA and 1.08 for PVP that are again considerably smaller of the value 5/3 for a Gaussian chain. The reason for these significant differences is concerned with intrachain interactions of the monomers and compaction influence of the water environment.
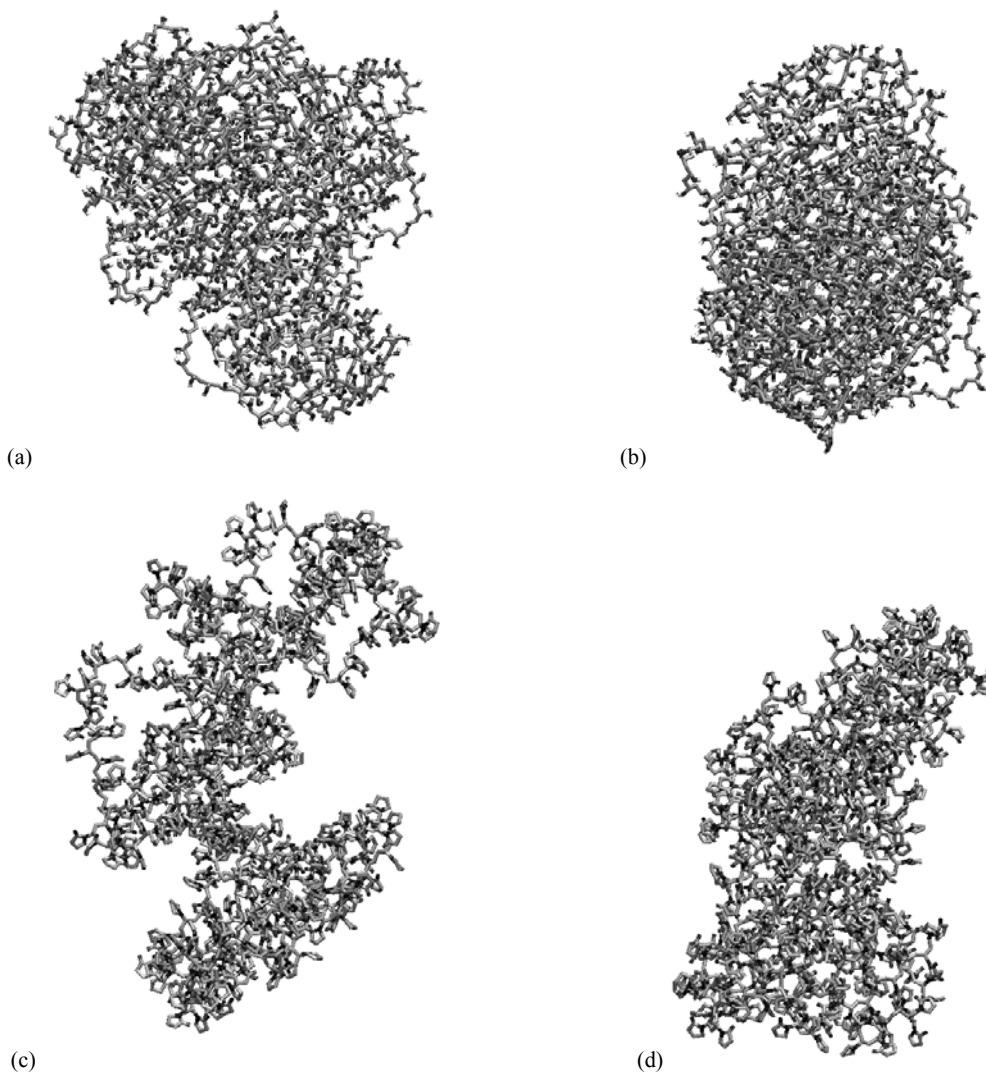

(a)

(b)

(c)

(d)

Fig. 2. Conformations of the PVA (a, b) and PVP (c, d) molecules for biological time t=0 (a, c) and t=100 ns (b, d)
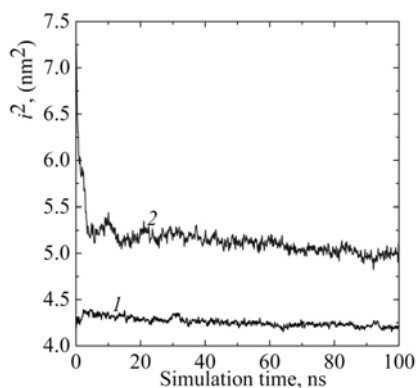

Fig. 3. The squared radius of gyration of the PVA (line 1) and PVP (line 2) molecules versus simulation time
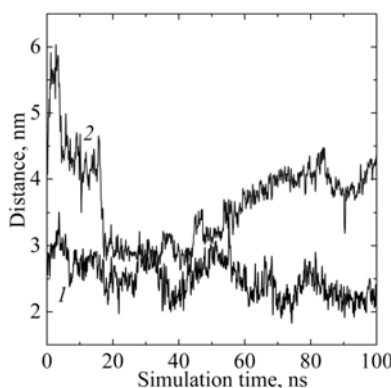
Fig. 4. The end to end distance of the PVA (line 1) and PVP (line 2) molecules

The shape of the polymers can be characterized by their principal moments of inertia or gyration radiuses. The PVA molecule is close to a spherical body with slightly diffused boundaries. Its radius can be estimated by the expression

$r = \sqrt{5/3}R_g \approx 1.29R_g$. One of the principal gyration radii of the PVP molecule is considerably larger of the two others.

A crude estimation of the semiprincipal axes of the PVP molecule can be written as

$$a \approx b \approx (\sqrt{5/2})R_z \;\square\; 1.58\sqrt{I_{zz}/m} \qquad (4),$$

and

$$c \approx \sqrt{(5/2)(I_{xx}^2 + I_{yy}^2 - I_{zz}^2)} \;\square\; 1.58\sqrt{(I_{xx}+I_{yy}-I_{zz})/m} \;\square\; 2.24\sqrt{(I_C - I_{zz})/m} \qquad (5),$$

where z axis lies along the longest ellipsoid semiaxis and $I_C = mR_g^2$.

The mean densities of the PVA and PVP water solutions are estimated as 0.97 and 0.94 g/cm^3, respectively, while the mean densities of these molecules themselves are found to be 1.14 and 0.954 g/cm^3. The experimental value of the pure amorphous PVA is 1.26 g/cm^3 [21]. The difference between the PVA densities can be attributed to diffuse boundary of the globule in our simulation.

Static correlations in the PVA and PVP molecules. The monomer units consist of quite rigid triangles with C–C–O or C–C–N nucleus in their vertexes. These triangles can be used for generation of the orthonormal bases (*Fig. 5*) to trace the conformation changes of the polymers. The ort **k** is aligned with C–C bond of the monomer. The ort **j** belongs to C–C–O or C–C–N planes in such a way that C–O or C–N bonds are disposed between **k** and **j** vectors. Ort **j** is calculated in accordance with the expression:

$$\mathbf{j} = \frac{\mathbf{l} - \mathbf{k}\cos\alpha}{\sin\alpha} = \frac{\mathbf{l} - \mathbf{k}(\mathbf{l}\cdot\mathbf{k})}{\sqrt{1 - (\mathbf{l}\cdot\mathbf{k})^2}}.$$

Fig. 5. The scheme of the orthonormal basis

The third ort **i** is determined by the vector product **i**=**j**×**k**.

Mutual orientation of C–C bonds of different monomers in the molecule can be characterized by the angle θ between the bonds. It can be calculated from the expression: $\cos\theta = \mathbf{k}\cdot\mathbf{k}'$ (7), where vectors **k** and **k'** belong to different monomers. The backbone was split into 200 monomers and cosθ between the first and all the other monomers was averaged over all the pieces. The averaging results are presented in *Fig. 6*. The correlation function becomes about zero on the distance of approximately 10 monomers. This feature can be considered as a persistent length of the PVA polymer at given thermodynamic conditions. Well pronounced periodic character of <cos θ> is observed at longer intermonomer distances.

The rigidity of the backbone can be characterized by the angle α between adjacent C–C bonds in the polymer. The α angle values as a function of monomer number is shown in *Fig. 7*. Due to the thermal motion this angle fluctuates around the 70° value, which is the equilibrium value in the monomer unit.

The mutual orientation of the triangle C–C–O or C–C–N planes is described by the angle between vectors **i** and **i'** belonging to different monomers. *Fig. 8* demonstrates that the mean value of the scalar product of vectors *i* and *i'* is close to zero. Thus, one can suggest that there is no correlation between orientations of C–C–O or C–C–N planes of different monomers even for neighboring monomer units. Thus, the monomers are able to rotate easily around C–C bonds.

Diffusion properties. The center of mass (tracer) diffusion coefficient D_{tr} can be calculated with the expression:

$$D_{tr} = \left\langle (\Delta\mathbf{r}_C)^2 \right\rangle \Big/ 6t, \qquad 8)$$

where $<(\Delta\mathbf{r}_C)^2>$ is the mean square displacement of the center of mass of the polymer, t is the simulation time.

For better statistics the polymers center of mass trajectories were divided into a number of partially overlapped pieces. The mean square center of mass displacements have been averaged over 980 trajectories by shifting of 20 ns window each time by 1 ns (*Fig. 9*).

The center of mass diffusion coefficients are given as a function of different piece lengths (*Fig. 10*). The pieces were overlapped by shifting the window by 1, 2, 4, 5, 10 or 20 ns depending on the piece length.
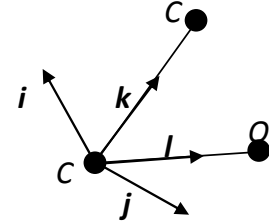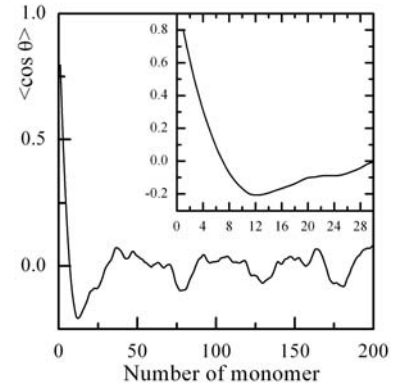
Fig. 6. Average cosθ versus intermonomer distance (in units of C–C bond) along the backbone for the PVA molecule
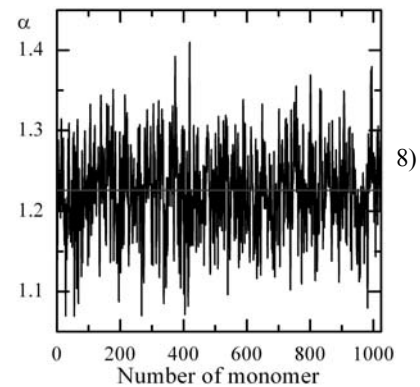
Fig. 7. Angle α versus intermonomer distance (in units of C–C bond) along the backbone for the PVA molecule

For the PVA molecule the values of the diffusion coefficient are scattered between 0.016 and 0.047 nm²/ns values. Thus, one can take D_{tr} =0.035 nm²/ns (or 3.5·10⁻¹¹ m²/s) value as the best estimate of the diffusion coefficient. The scatter is considerably bigger for the PVP molecule. However, the results are close to 0.01 nm²/ns for trajectories of 10 to 20 ns length.

The center of mass diffusion coefficients of the PVA and PVP molecules are almost independent on the time shift (*Fig. 11*). However, the increase in the time shift (the decrease in the number of the trajectories) leads to increase in the noise level of the mean trajectories. According to Langevin equation and the fluctuation-dissipation theorem the relaxation time of the momentum (or the center of mass velocity) is given by the expression [22]:

$$\tau_p = mD_{tr} / k_B T \qquad ,$$

where m is the molecule mass, k_B Boltzmann constant, T absolute temperature. The relaxation time has been calculated for the PVA molecule ($m=7.48·10^{-23}$ kg) $\tau_p \approx 0.6$ ps. Based on this value the memory effects can be neglected for trajectories larger than 0.1 ns. For the PVP molecule the relaxation time was found to be even shorter, 0.2 ps.

To investigate the rotation of polymers the direct integration of the differential equation of rotational motion cannot be used. The main problem is that polymers are not rigid compounds. Therefore, it is necessary to link the polymer molecule with a coordinate system, which would describe its rotational movement. One of such possibilities consists in the equating of the angular momentum of the polymer in the center of mass coordinate system, with that of a rigid body

$$\mathbf{J}_C \cdot \boldsymbol{\omega} = \sum_k m_k \mathbf{r}_k \times \mathbf{v}_k \qquad ,$$

where $\mathbf{J}_C$ is the moment of inertia tensor defined through masses and coordinates of all the atoms

$$\mathbf{J}_C = \begin{pmatrix} \sum_k m_k \left(y_k^2 + z_k^2 \right) & -\sum_k m_k x_k y_k & -\sum_k m_k x_k z_k \\ -\sum_k m_k x_k y_k & \sum_k m_k \left(x_k^2 + z_k^2 \right) & -\sum_k m_k y_k z_k \\ -\sum_k m_k x_k z_k & -\sum_k m_k y_k z_k & \sum_k m_k \left(x_k^2 + y_k^2 \right) \end{pmatrix} ,$$

$\boldsymbol{\omega}$ is the rotational velocity of the associated coordinate system that can be considered as the mean rotational velocity of the molecule, $m_k, \mathbf{r}_k, \mathbf{v}_k, x_k, y_k, z_k$ are the mass, radius-vector, velocity and coordinates of k-th atom of the molecule, correspondingly, which are calculated in the polymer center of mass coordinate system with fixed orientation.

Eq. (10) can be rewritten as

$$\mathbf{J}_C \cdot \frac{d\boldsymbol{\varphi}}{dt} = \sum_k m_k \mathbf{r}_k \times \frac{d\mathbf{r}_k}{dt}, \qquad (12)$$

and after reduction of dt the expression for the infinitesimal mean angle of rotation acquires the following form:

$$\mathbf{J}_C \cdot d\boldsymbol{\varphi} = \sum_k m_k \mathbf{r}_k \times d\mathbf{r}_k . \qquad (13)$$

The mean angle of molecular rotation at small time step is given by the approximate expression:

$$\Delta\boldsymbol{\varphi} \cong \mathbf{J}_C^{-1} \cdot \sum_k m_k \mathbf{r}_k \times \Delta\mathbf{r}_k . \qquad (14)$$

This definition is reasonable, when the moment of inertia tensor does not significantly change during each time step. After N time steps the rotation angles around the coordinate axes are determined by the sums over the time steps
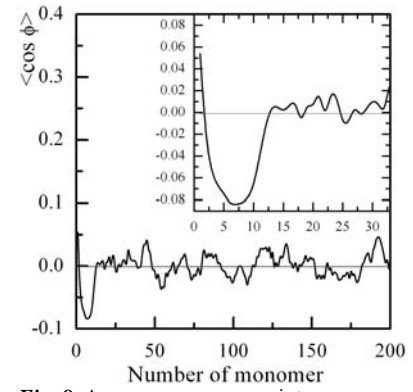

Fig. 8. Average cosφ versus intermonomer distance (in units of C–C bond) along the backbone for the PVA molecule
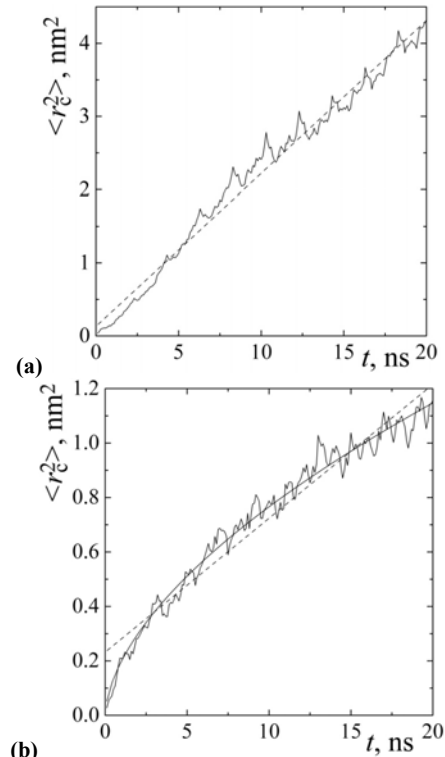
(9)

(a)

(b)

Fig. 9. The mean square center of mass displacements averaged over 41 trajectories of 20 ns duration for the PVA (a) and PVP (b) molecules. The dashed lines are linear fittings, the full line is a square root fitting

$$\Delta\varphi_x(t) = \sum_{\tau=1}^{N} \Delta\varphi_x^{\tau}\Delta t, \quad \Delta\varphi_y(t) = \sum_{\tau=1}^{N} \Delta\varphi_y^{\tau}\Delta t, \quad \Delta\varphi_z(t) = \sum_{\tau=1}^{N} \Delta\varphi_z^{\tau}\Delta t, \qquad (15)$$
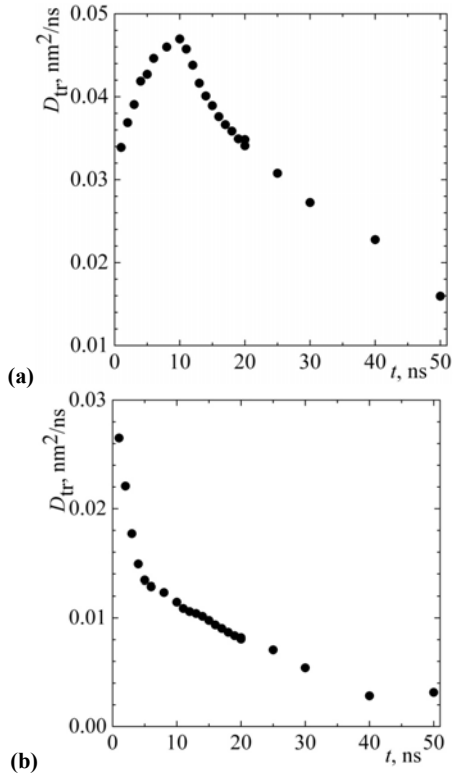
(a)

(b)

Fig. 10. The PVA (a) and PVP (b) tracer diffusion coefficients estimated from the trajectories of different piece lengths
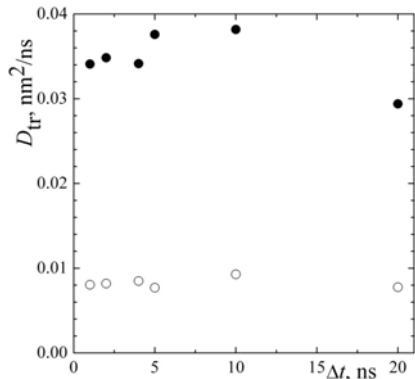
Fig. 11. The translational diffusion coefficients versus the time shift for trajectories of 20 ns duration for the PVP (open circles) and PVA (full circles) molecules

where Δt is the time step duration. The mean square angular displacement during time $t=N\Delta t$ is a sum of the mean square rotations around the coordinate axes of the center of mass system with fixed orientation of the axes.

$$\left(\Delta\varphi(t)\right)^2 = \left(\Delta\varphi_x(t)\right)^2 + \left(\Delta\varphi_y(t)\right)^2 + \left(\Delta\varphi_z(t)\right)^2.$$

The rotational diffusion coefficient can be introduced as

$$D_{\text{rot}} = \left\langle (\Delta\varphi)^2 \right\rangle \big/ 6t.$$

The results for the rotational diffusion coefficients of the PVA and PVP polymers as a function of different trajectory piece lengths are represented in *Fig. 12*.

Again, the results for trajectories of 20 ns duration are most appropriate from the point of view of good statistics and trajectory duration. Thus the rotational diffusion coefficients for the PVA and PVP molecules can be estimated as 0.01 and $7\cdot10^{-6}$ (rad)^2/ps, respectively. The examples of the rotation mean square angles are shown in *Fig. 13*.

Since the geometric molecular characteristics of the polymers have been estimated it is advisable to compare the molecular dynamics results with the hydrodynamic estimations.

For the PVA molecule, the shape of which is close to a sphere, the hydrodynamic value of the center of mass diffusion coefficient is:

$$D_{\text{tr}} = k_{\text{B}}T / (6\pi r\eta) \,\square\, 1{,}03\cdot10^{-10}\,\text{m}^2/\text{s}=0.103\,\text{nm}^2/\text{ns},$$

where $\eta=8{,}5\cdot10^{-4}$ Pa·s is the viscosity of water at 300 K and $r = 1{,}29\,r_g \approx 2{,}5$ nm is the molecule radius. The rotational diffusion coefficient is given as:

$$D_{\text{rot}} = k_{\text{B}}T / (8\pi r^3\eta) \,\square\, 0.012\,(\text{rad})^2/\text{ps}.$$

For the PVP molecule the longest axis is 8.1 nm and the short axes are around 4.3 nm. The aspect ratio p is 8.1/4.3=1.9. The average translational friction coefficient is [23]

$$f_{\text{tr}} = 3\pi L\eta\sqrt{p^2-1} / p\ln(p+\sqrt{p^2-1}) \,\square\, 4.4\cdot10^{-11}\,\text{kg/s}$$
,

and the center of mass diffusion coefficient

$$D_{\text{tr}} = k_{\text{B}}T / f_{\text{tr}} \,\square\, 0{,}94\cdot10^{-10}\,\text{m}^2/\text{s}=0.094\,\text{nm}^2/\text{ns}$$

that is almost the same value as for the PVA molecule.

The friction coefficient for rotation around the axis perpendicular to the longest ellipsoid axis at $p\gg1$ (p^2-1 and p^4-1 enter in the exact equation, thus $p=1.9$ can be considered as a big value) is given by the expression [24, 25]:

$$f_{\text{rot}} \,\square\, \pi\eta L^3 / 3(\ln 2p - 0.5) \cong 5.7\cdot10^{-28}\,\text{kgm}^2/\text{s},$$

and the hydrodynamic estimation of the rotational diffusion coefficient leads to the value

$$D_{\text{rot}} = k_{\text{B}}T / f_{\text{rot}} \,\square\, 0.9\cdot10^7\,(\text{rad})^2/\text{s}=0.009\,(\text{rad})^2/\text{ns}.$$

Thus, the hydrodynamic estimations of the translational as well as rotational diffusion coefficients for the PVA and PVP molecules are close to each other because their linear dimensions are comparable. On the other hand, the MD estimations for the diffusion coefficients of these molecules significantly differ, and deviate also from the hydrodynamic estimations. The MD value of the PVA rotational diffusion coefficient is close to its hydrodynamic estimation only, while the other MD values of the diffusion coefficients are significantly smaller compared to the hydrodynamic estimations. For example, the MD estimation of the PVA translational diffusion coefficient is three times smaller than its hydrodynamic value and for the PVP molecule the difference is almost an order of magnitude. Especially large deviation was found for the PVP rotational diffusion coefficient.
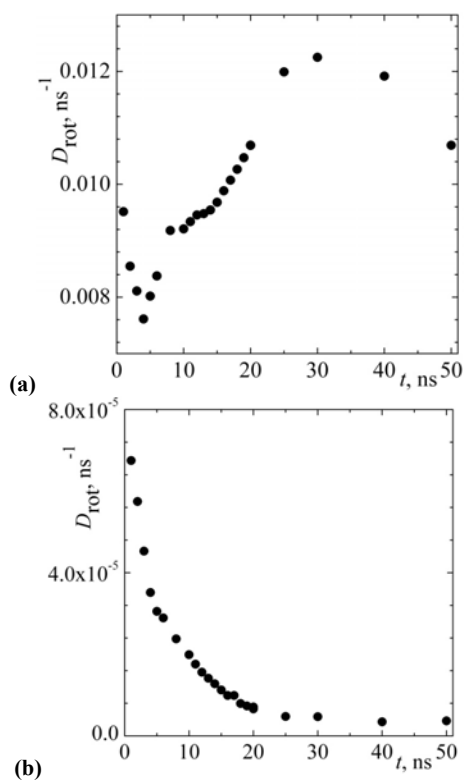
(a)

(b)

Fig. 12. The PVA (a) and PVP (b) rotational diffusion coefficients estimated from trajectories of different piece lengths
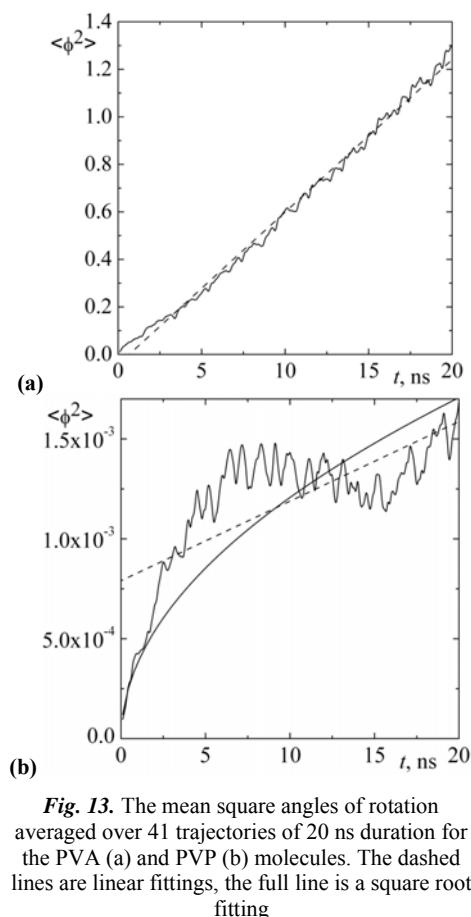

(a)

(b)

Fig. 13. The mean square angles of rotation averaged over 41 trajectories of 20 ns duration for the PVA (a) and PVP (b) molecules. The dashed lines are linear fittings, the full line is a square root fitting

There are several reasons for the discrepancies between MD and hydrodynamic estimation results. First of all, the polymer surfaces are not smooth and the surface monomers move each with respect to others. Thus, the polymer–water interactions can significantly differ from their hydrodynamic estimations and correspondingly the diffusion coefficients values can strongly deviate from the hydrodynamic estimations. Although statistics needs to be improved, from *Figs. 9–13* it follows that better statistics can change the real coefficients values around several tens percent only, especially for the coefficients of translational diffusion. One more reason concerns the MD simulation box size because its edge is around 10 nm that is slightly longer than PVA and PVP globules size. The latter is especially important for the PVP molecule with its longest ellipsoid axis around of 8 nm because their synchronized motion in the adjacent simulation boxes due to the periodic boundary conditions can significantly violate the surrounding water hydrodynamic fluxes and increase the hydrodynamic friction. To estimate the effect of the simulation box size on the diffusion coefficients estimation it is necessary to perform the simulation with different box sizes.

Nevertheless, we have to conclude that the conformation and dynamic properties of the PVA and PVP molecules significantly differ. First of all, the PVA and PVP molecules strongly differ in their shapes. The PVA molecule is close to a spherically symmetric body while the PVP molecule is angularly-shaped and cannot be considered as an ellipsoid of revolution. Therefore, the PVP rotational diffusion coefficient is more than three orders of magnitude smaller as compared to that of the PVA molecule. Moreover, the difference exists not only in the numerical values; some qualitative characteristics differ as well. For the PVA molecule the mean square center of mass displacement as well as the mean square angles of rotation linearly depends on time (*Figs. 9a, 13a*) and its diffusion can be considered as ordinary one. This is not the case for the PVP molecule (*Figs. 9b, 13b*) where the mean square deviations are characteristic for subdiffusion behavior $\left\langle (\Delta \mathbf{g})^2 \right\rangle \propto t^{\alpha}$, $\mathbf{g} = \mathbf{r}_C, \boldsymbol{\varphi}$ with $\alpha \cong 0.5$.

The results for 20 ns trajectories are shown in *Figs. 9, 13*. For the trajectories from 10 to 30 ns similar results are observed. This subdiffusion behavior can be the main reason for strong difference between the diffusion characteristics of the PVA and PVP molecules when they are considered as ordinary diffusion for both of them.

CONCLUSION

The MD simulation results show that the properties of the PVA and PVP molecules are significantly different. Both molecules demonstrate globular structure but the PVA molecule is close to a spherically symmetric body while the PVP molecule is angularly-shaped. The mean density of the molecules estimated through the radius and the ellipsoid axes is equal to $1.1 \cdot 10^3$ and $0.96 \cdot 10^3$ kg/m³ for the PVA and PVP molecules, correspondingly, i.e. the density of the PVP molecule is significantly smaller because of its bulky monomers resist stronger to the compaction process. The ratio of the end-to-end distance to the gyration radius for both polymer molecules is considerably smaller than the value estimated for the Gaussian chains. The correlation between orientations of C–C bonds along the polymer backbone disappears on the distance of several C–C bonds.

Diffusion behavior of the polymers is qualitatively different. The

PVA translational and rotational motions obey ordinary diffusion, while the PVP molecule shows subdiffusion regime with the exponent around of 0.5. As a result, the PVP molecule is considerably less mobile on the time scale considered. The comparison of the MD simulation results with hydrodynamic estimations shows that the hydrodynamic theory underestimates the friction characteristics of the PVA molecule and is not applicable to the PVP molecule at all.

REFERENCES

[1] M.P. Stevens, *Polymer Chemistry: an Introduction* (Oxford University Press, Oxford, 1990).
[2] E. Chiellini, R.M. Ottenbrite, *Polymers in Medicine: Biomedical and Pharmaceutical applications* (CRC Press, 1992).
[3] A.A. Shahinian *et al.*, *Proc. of the Armenia Acad. of Scien., physics*, **15**, 55 (1980).
[4] V. Bühler, *Polyvinylpyrrolidone Excipients for Pharmaceuticals: Povidone, Crospovidone and Copovidone*, (Springer-Verlag Berlin, Heidelberg, 2005).
[5] C.A. Finch (ed.), *Polyvinyl alcohol – Developments*, (Wiley, Chichester and New York, 1992).
[6] M. Kobayashi *et al.*, *Biomaterials*, **24**, 639 (2003).
[7] G. Tesei *et al.*, *J. Phys. Chem. B*, **116**, 10008, (2012).
[8] E. Rossinsky *et al.*, *Macromolecular Theory and Simulations*, **18**, 545 (2009)
[9] G. Paradossi *et al.*, *Polymers*, **3**, 1805, (2011)
[10] K. Bjorn *et al.*, *Molecular Physics*, **90,** 979, (1997)
[11] T.X.Xiang *et al.*, *J. Pharm. Sci.,* **102,** 876, (2012)
[12] G. Tesei *et al.*, *J. Phys. Chem. B*, **33**, 10008 (2012).
[13] W.L. Jorgensen *et al.*, *J. Chem. Phys.*, **79**, 926 (1983).
[14] B. Hess *et al., GROMACS Groningen Machine for Chemical Simulations. User Manual. Version 4.5.4* (University of Groningen, Nijenborgh, 2011).
[15] H.J.C. Berendsen *et al.*, *J. Chem. Phys.*, **81**, 3684 (1984).
[16] G. Bussi *et al.*, *J. Chem. Phys.*, **126**, art. no. 014101 (2007).
[17] T. Darden *et al.*, *J. Chem. Phys.*, **98**, 10089 (1993).
[18] T. Schlick, *Molecular Modeling and Simulation: an Interdisciplinary Guide* (Springer Science + Business Media, New York, 2010).
[19] B. Hess *et al.*, *J. Comp. Chem.*, **18**, 1463 (1997).
[20] P.J. Flory, *Statistical Mechanics of Chain Molecules* (Wiley–Interscience publishers, New York, 1969).
[21] R.L Davidson, *Handbook of Water-Soluble Gums and Resins* (MacGraw-Hill, New York, 1980).
[22] N.G. van Kampen, *Stochastic Processes in Physics and Chemistry* (Elsevier, Amsterdam, 1992).
[23] F. Perrin, *J. Phys. Radium.*, **7**, 1 (1936).
[24] F. Perrin, *J. Phys. Radium.*, **5**, 495 (1934).
[25] S. Koenig, *Biopolymers*, **14**, 2421 (1975).